

A Robust and Automated Method for Estimating the Expected Signal Standard Deviation in DWI Datasets

Lin-Ching Chang¹, and Carlo Pierpaoli²

¹Department of Electrical Engineering and Computer Science, The Catholic University of America, Washington, DC, United States, ²National Institutes of Health, Bethesda, MD, United States

Introduction: Correctly estimating the expected signal standard deviation (SD) due to thermal noise in diffusion weighted images (DWIs) is important. For examples, for identical acquisition parameters, signal SD reflects the performance of the MR hardware system [1]. Knowledge of signal SD is required for image processing tasks such as image registration and filtering [2]. It is also needed to correctly compute the chi-squares value for the measurement of goodness of fit for tensor estimation [3], to estimate the reproducibility of measured quantities [4], and to detect outliers in DWIs [5, 6]. For classical single channel acquisitions, signal SD could be estimated from a ghost-free region of the image background [1]. However, the signal in the background of DWIs acquired on modern clinical scanners cannot be used for this purpose because of the effects of signal processing and filtering applied during image reconstruction in data acquired with parallel imaging techniques. One could extract signal SD on a voxel-wise basis from a large number of replicates. However, acquiring replicated images is time consuming and it is rarely done only for the purpose of measuring signal SD. Here we propose a practical method for extracting signal SD from the acquired DWIs, eliminating the need for acquiring replicated images. This method takes advantage of robust regression and residual analysis of the tensor fitting using the median absolute deviation of the residuals to estimate signal SD. Monte Carlo simulations were used to validate the proposed method and to compare to an existing signal SD estimation method (i.e., Walker's method) that uses a collection of reduced chi-squares values measured in the object [7].

Methods: Let us denote s_{ijk} as the residual standard deviation at voxel location (i, j, k) . Using the residuals obtained from the fitting, we can estimate s_{ijk} based on a robust scalar estimator such as the median absolute deviation (MAD).

$s_{ijk} = \text{median}\{|r_1 - \tilde{r}|, |r_2 - \tilde{r}|, \dots, |r_n - \tilde{r}|\}$, where n is the no. of data points, r_i are the residuals, and \tilde{r} is the median of the residuals. Based on the value of s_{ijk} , we then can estimate the value of $\hat{\sigma}_{ijk}$, the expected signal standard deviation at voxel location (i, j, k) , using the following formula.

$$\hat{\sigma}_{ijk} = \sqrt{n/(n-p)} \times s_{ijk}, \text{ where } n \text{ is the no. of data points and } p \text{ is 7 for the unknown parameters in tensor estimation.}$$

Using the sample median of a collection of $\hat{\sigma}_{ijk}$, we obtained the robust estimation of signal SD for the dataset. We denote the method derived from the residual analysis using MAD as RMAD. Although RMAD improves Walker's method, it does not fully address the situation of one or more bad volumes in the dataset. To solve this problem, we add an additional step before the residual analysis. We perform robust regression using the Geman-McClure M-estimator [8] and remove a certain percentage of voxels based on a user-defined parameter, i.e., the user specifies the percentage of data to remove before tensor fitting and residual analysis. We denote the method using robust regression and residual analysis using MAD as RRMAD. Monte Carlo simulations using synthetic human brain data similarly to what is described in [9] were used to evaluate and compare the effectiveness of the proposed methods. Datasets were created using Jones' 30 direction scheme [10] with $b=1000 \text{ s/mm}^2$ and 5 $b=0$ images. Gaussian-distributed noise in quadrature was added to simulate images with the true signal SD = 500, i.e., an SNR of 20 measured in the thalamus of the $b=0$ image. We then corrupted one, two, or three images of the dataset by multiplying the original signal intensity by a factor ranging from 0.30 to 1.70.

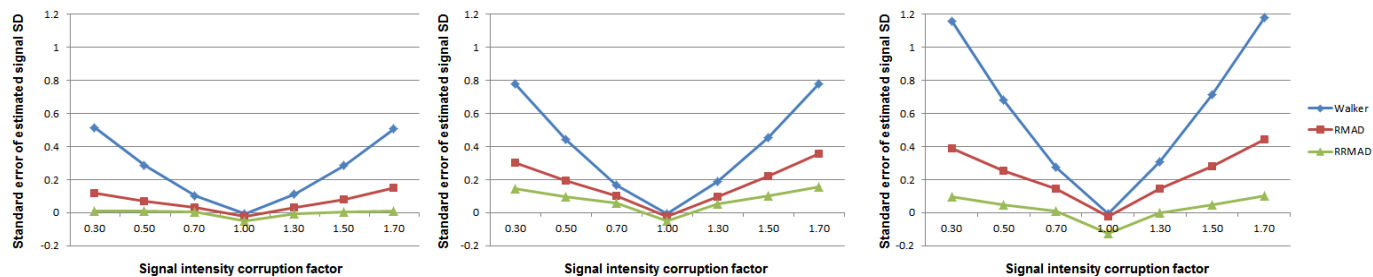


Fig. 1 The standard error of computed signal standard deviation using the Walker, RMAD, and RRMAD methods with (a) one, (b) two, and (c) three corrupted images. The corrupted signal intensity values are set to be the original signal intensity values multiplied by the signal intensity corruption factors ranging from 0.30 to 1.70 that simulated different types and severity levels of artifacts.

Results and Discussion: Figure 1 shows the standard error of estimated signal SD using the Walker, RMAD, and RRMAD methods. The standard error is defined as the ratio of estimated signal SD minus true signal SD, divided by the true signal SD. Walker's method did not perform well in the presence of artifacts with the standard error over 50% in the case of a single corrupted volume and about 80% and 120% in the case of two and three corrupted volumes, respectively. The RMAD method improved the signal SD estimation, and RRMAD outperformed the Walker and RMAD methods regardless of the types and the severity levels of artifacts. Note that when there are no artifacts in the data set, the Walker and RMAD methods perform better than RRMAD; RRMAD results in a slightly underestimated signal SD. The standard error, however, is acceptable within about 3%, 5%, and 10% underestimation of signal SD for the case of one, two, and three corrupted volumes, respectively. This situation arises because even when the dataset is free of artifacts, the RRMAD method still identifies points in the tail of the residual distribution as outliers and removes them from the fitting.

Conclusions: The proposed method is fully automated and very robust, even in the presence of DWI volumes which are completely corrupted. Although we applied the method to DWI datasets, it can be applied to other imaging modalities when fitting signal data to estimate quantitative parameters such as T1 and T2 relaxation times.

References: [1] Henkelman, RM, Medical Physics, 1985. **12**(2): p. 232-233. [2] Rohde, GK, et al., Magn Reson Med, 2004. **51**(1): p. 103-14. [3] Basser, PJ, et al., J Magn Reson B, 1994. **103**(3): p. 247-54. [4] Jones, DK, et al., Magn Reson Med, 2004. **52**(5): p. 979-93. [5] Chang, L-C, et al., Magn Reson Med, 2005. **53**(5): p. 1088-95. [6] Chang, L-C, et al., ISMRM 19th Ann. Meeting, pp. 3898, 2011. [7] Walker L, et al., Neuroimage 2011;54(2):1168-1177. [8] Bevington P, McGraw-Hill Book Company, 1969. [9] Chang, L-C, et al., Magn Reson Med, 2007;57(1):141-149. [10] Jones DK, et al., Magn Reson Med 1999;42(3):515-525.